PHYSICAL REVIEW B VOLUME 9, NUMBER 2 15 JANUARY 1974

Phonon focusing and phonon conduction in hexagonal crystals in the boundary-scattering regime

A. K. McCurdy
Electrical Engineering Department, Worcester Polytechnic Institute, Worcester, Massachusetts 01609
(Received 15 March 1973)

Striking differences (up to factors of several hundred) are predicted in the intensity of phonons propagating ballistically along different directions to the c axis in certain hexagonal crystals. The predicted results arise from phonon focusing, due to the fact that in elastically anisotropic crystals the phonon phase and group velocities are, in general, not collinear. Analytic expressions have been derived for the amplification factor for phonons of each polarization along all directions where the phase and group velocities are collinear. Calculations have been performed for a number of hexagonal crystals and demonstrate that the phonon-focusing property can effect differences in the phonon transport in the boundary-scattering regime by as much as 300%.

I. INTRODUCTION

In dielectric solids thermal energy is carried by quantized elastic waves or phonons. At sufficiently low temperatures the phonons propagate ballistically rather than diffusely, so that the phonon mean free path becomes limited by geometrical-scattering processes.[1] In the absence of impurity or defect scattering, the phonon mean free path becomes limited by the linear dimensions of the sample. A theory of the thermal conductivity κ applicable to this temperature range was first developed by Casimir,[2] whose result may be expressed in the following equivalent forms:

$$\kappa = (2\pi^2 k_B^4/15\hbar^3)\langle s^{-2}\rangle \Lambda_c T^3 , \tag{1}$$

$$\kappa = \tfrac{1}{3} C_v(\langle s^{-2}\rangle/\langle s^{-3}\rangle)\Lambda_c , \tag{2}$$

where $\langle s^{-2}\rangle$ and $\langle s^{-3}\rangle$ are, respectively, averages of the inverse square and inverse cube of the phonon phase velocity, T is the temperature, and C_v the specific heat per unit volume. The Casimir length Λ_c may be regarded as the effective phonon mean free path. For a circular cross-section rod, Λ_c is equal to the rod diameter and for a square rod of side D

$$\Lambda_c = 1.115D . \tag{3}$$

Casimir assumed that the walls of the sample acted as diffuse scatterers of phonons (i.e., a phonon striking the surface of the crystal would be reradiated with random direction) and that the sample length is very much greater than its transverse dimension. Corrections to Casimir's theory have been derived by Berman and co-workers for samples with a finite ratio of length to width[3] and for samples in which a fraction of the phonons are specularly reflected from the side and end surfaces.[4]

Recent heat-pulse measurements[5,6] have shown that when phonons are excited in a given region of an elastically anisotropic crystal, the energy flow will be enhanced or focused in some directions and decreased in others even if the angular distribution of wave vectors is uniform. This enhancement or decrease arises because the group velocity $\vec{v}$ is not generally in the same direction as the wave vector $\vec{k}$ or the phase velocity $\vec{s}$. The amount of energy received by a heat-pulse detector depends upon the phonon polarization and the crystallographic direction between the generator and the detector. The energy received varies for the different phonon polarizations because the deviation between the wave vector and corresponding group velocity is different for each polarization.

Calculations to determine the relative intensities of phonons for each polarization were previously carried out for a number of cubic crystals[6] and the results are listed elsewhere.[6,7] The phonon densities were also calculated using an analytic expression derived for cubic crystals by Maris.[8] The same large differences (up to factors of 100) were predicted by both methods and observed experimentally in the intensity of phonons of different polarizations propagating along different crystallographic directions.[5,6]

Subsequent measurements of the thermal conductivity of silicon and calcium fluoride in the boundary-scattering regime demonstrated a pronounced anisotropy.[9] The conductivity was found to depend upon the orientation of the sample rod axis, the variation being as much as 50% for silicon and 40% for calcium fluoride. This anisotropy was explained in terms of phonon focusing arising from elastic anisotropy. The thermal conduction was found to be higher when the heat-flow axis was parallel to a crystallographic direction in which the energy flow was enhanced or focused.

At temperatures much less than the Debye temperature most of the thermal energy of a solid is

contained in the transverse modes because of their lower velocity. Since the thermal conductivity at these low temperatures is approximately inversely proportional to the square of the phonon velocity, the transverse modes, because of their lower velocity, will make the major contribution to the flow of heat. Energy flow in such a solid was enhanced along those crystallographic directions in which the transverse modes were most strongly focused and de-enhanced along those directions where these modes were strongly defocused. Thermal conduction in the boundary-limited regime was thus larger than the Casimir value when the sample rod axis was parallel to a direction in which the energy flow was enhanced, and smaller than the Casimir value along those directions where the energy flow was decreased.

Casimir's theory of thermal conduction in the boundary-scattering regime was generalized to include the effects of phonon focusing. Corrections to the thermal conductivity were derived for samples of finite length. The predictions of this generalized theory were in quantitative agreement with experimental results.

In metals, however, most of the thermal energy is carried by electrons so that the thermal conductivity at low temperatures is dominated by electrons and not phonons. In those metals which undergo a superconducting transition, thermal transport is dominated at the highest temperatures below the transition by normal-state electrons. As the temperature is reduced electrons condense into the superconducting state pairing with electrons of opposite spin and wave vector.[10] The thermal energy carried by electrons thus decreases as more normal-state electrons become Cooper pairs. Far below the transition temperature T_c, i.e., $T/T_c \ll 1$, the electronic scattering of phonons and the thermal energy carried by normal-state electrons decreases until thermal transport is completely dominated by boundary-scattered phonons. Thus for $T/T_c \ll 1$ the thermal conductivity of a pure defect-free superconductor should approach the value predicted from elastic anisotropy in a dielectric crystal. These remarks appear substantiated by recent measurements on the thermal conductivity of pure niobium from 0.04 to 4 °K which indicate that the thermal conductivity at the lowest temperatures is dominated by the boundary scattering of phonons.[11]

In this paper analytic expressions are derived for the phonon amplification resulting from phonon focusing in hexagonal crystals. Conditions for focusing are derived for phonons of each polarization along all directions where the phase and group velocities are collinear. Conditions are also derived for the existence of cuspidal edges in the group-velocity surfaces about these same directions. Calculations of phonon focusing are given for a number of hexagonal crystals, including a number of superconductors. Strong phonon focusing is predicted to have a dramatic effect upon the phonon conductivity at very low temperatures. For dielectric solids this should be observable at temperatures that are a small fraction of the Debye temperature, but for superconductors this will not likely be observed until $T/T_c \ll 1$.

II. THEORY

A. Calculation of phonon phase and group velocities

The solutions for the phonon phase velocities in the hexagonal elastic solid are well known[12-14]:

$$s_1^2 = (C_{66}\sin^2\theta_k + C_{44}\cos^2\theta_k)/\rho\,, \tag{4}$$

$$s_{0,2}^2 = \frac{1}{2\rho}\{(C_{11}+C_{44})\sin^2\theta_k + (C_{33}+C_{44})\cos^2\theta_k \pm[((C_{11}-C_{44})\sin^2\theta_k - (C_{33}-C_{44})\cos^2\theta_k)^2 + (2(C_{13}+C_{44})\sin\theta_k\cos\theta_k)^2]^{1/2}\}\,. \tag{5}$$

The displacement vector $\vec{u}$, giving the direction of the deformation, is given by[14]

$$\vec{u}_1 = \frac{\vec{e}\times\vec{n}}{[1-(\vec{e}\cdot\vec{n})^2]^{1/2}}\,, \tag{6}$$

$$\vec{u}_{0,2} = \vec{n} - \left(\frac{[(C_{11}-C_{44})\sin^2\theta_k - (C_{33}-C_{44})\cos^2\theta_k] + 2(C_{13}+C_{44})\cos^2\theta_k}{2(C_{13}+C_{44})\cos\theta_k} \mp \frac{\{[(C_{11}-C_{44})\sin^2\theta_k - (C_{33}-C_{44})\cos^2\theta_k]^2 + [2(C_{13}+C_{44})\sin\theta_k\cos\theta_k]^2\}^{1/2}}{2(C_{13}+C_{44})\cos\theta_k}\right)\vec{e}\,. \tag{7}$$

In these equations s is the phase velocity, C_{ij} is the second-order elastic constants, θ_k is the angle of the wave vector relative to the C axis, $\vec{n}$ is a unit vector in the direction of the wave vector, and $\vec{e}$ is a unit vector parallel to the C axis. The subscripts 0, 1, 2 on the phase velocity and the displacement vector refer to the different modes of propagation which will be designated as the fast, transverse T_1, and slow modes, respectively. The sign preceding the radical is positive for the fast mode and negative for the slow mode in Eq. (5), but is negative for the fast mode and positive for

the slow mode in Eq. (7). From Eq. (7) it can be seen that if $C_{33} > C_{44}$ the fast mode is quasilongitudinal and the slow mode is quasitransverse near the C axis, but if $C_{44} > C_{33}$ the fast mode is quasitransverse and the slow mode is quasilongitudinal along these same directions. Similarly, if $C_{11} > C_{44}$ the fast mode is quasilongitudinal and the slow mode is quasitransverse along directions nearly perpendicular to the C axis ($C_\perp$ directions); but if $C_{44} > C_{11}$ the fast mode is quasitransverse and the slow mode is quasilongitudinal along these directions.[15] Although there appears to be no known hexagonal material for which either $C_{11} < C_{44}$ or $C_{33} < C_{44}$, one should not rule-out either possibility. The recent discovery that paratellurite,[16,17] a tetragonal piezoelectric crystal, has along the ⟨100⟩ direction a shear wave phase velocity which exceeds that of the longitudinal indicates that one of the above possibilities could exist for a hexagonal crystal. Furthermore, neither possibility is prohibited by conditions for elastic stability, namely,[18]

$$C_{11} > 0, \quad C_{11} > |C_{12}|, \quad C_{33} > 0, \quad C_{44} > 0, \quad C_{66} > 0,$$

and

$$C_{33}(C_{11} - C_{66}) > C_{13}^2 . \tag{8}$$

The components of group velocity parallel and perpendicular to the C axis, respectively, can be determined using the relations[19]

$$v_z = \frac{\partial s}{\partial(\cos\theta_k)}, \quad v_\perp = \frac{\partial s}{\partial(\sin\theta_k)} . \tag{9}$$

The direction of the group velocity, θ_v, can then be determined by the relation

$$\tan\theta_v = v_\perp / v_z . \tag{10}$$

The results for each mode are

$$\tan\theta_v = (C_{66}/C_{44})\tan\theta_k \quad \text{or} \quad \cot\theta_v = (C_{44}/C_{66})\cot\theta_k \tag{11}$$

for the T_1 mode and

$$\tan\theta_v = (u/v)\tan\theta_k , \tag{12}$$

where

$$u = (C_{11}+C_{44}) \pm \frac{(C_{11}-C_{44})^2\tan^2\theta_k + [2(C_{13}+C_{44})^2 - (C_{11}-C_{44})(C_{33}-C_{44})]}{\{[(C_{11}-C_{44})\tan^2\theta_k - (C_{33}-C_{44})]^2 + [2(C_{13}+C_{44})\tan\theta_k]^2\}^{1/2}} , \tag{13}$$

$$v = (C_{33}+C_{44}) \pm \frac{[2(C_{13}+C_{44})^2 - (C_{11}-C_{44})(C_{33}-C_{44})]\tan^2\theta_k + (C_{33}-C_{44})^2}{\{[(C_{11}-C_{44})\tan^2\theta_k - (C_{33}-C_{44})]^2 + [2(C_{13}+C_{44})\tan\theta_k]^2\}^{1/2}} , \tag{14}$$

and the + sign is used for fast waves and the − sign for slow waves. For directions nearly perpendicular to the C axis it is more convenient to use

$$\cot\theta_v = (u'/v')\cot\theta_k , \tag{15}$$

where u' is u and v' is v, respectively, but with $\cot\theta_v$ replacing $\tan\theta_v$, C_{11} replacing C_{33}, and C_{33} replacing C_{11}.

These equations enable one to calculate the angle between the phase and group velocities for each mode along all wave-vector directions with respect to the C axis. For elastically anisotropic crystals the phonon phase and group velocities are collinear for only certain directions determined by the symmetry and the kind of anisotropy. This is discussed in more detail in Sec. II B.

For certain ratios between the elastic constants it is possible to find values of θ_v for the slow mode which permit more than one corresponding value of θ_k. In these regions the values of θ_k can be double or triple valued and the group-velocity surface is said to have cuspidal edges (see Figs. 1–4). The conditions for which cuspidal edges occur are discussed in Sec. II D.

B. Calculation of collinear and pure-mode points

A collinear point will be defined as one in which the phase velocity or wave vector and the corresponding group velocity are collinear. At these points the flow of energy is in the same direction as the wave vector. A pure-mode point will be defined as one in which the displacement or polarization vector and the wave vector are either collinear (i.e., a pure longitudinal wave) or perpendicular (i.e., a pure transverse wave). Pure modes propagate in general only for wave vectors parallel and perpendicular to the C axis. Along these directions the wave vector and group velocity for all modes are collinear. Although the transverse T_1 wave is a pure mode for all directions of the wave vector, the group velocity and wave vector for this mode are collinear, in general, only for wave vectors parallel and perpendicular to the C axis. Solution for the collinear points for the fast and slow modes yields the values $\theta_k = 0°$ and 90° required by symmetry, as well as a quadratic equation in $\tan^2\theta_k$. The quadratic equation, which incidentally is identical for both the fast and slow modes, yields the roots

$$\tan^2\theta_k = \frac{(C_{13}+C_{33})}{(C_{13}+C_{11})} \quad \text{or}$$

$$\tan^2\theta_k = \frac{(C_{13}+C_{44}) - (C_{33}-C_{44})}{(C_{13}+C_{44}) - (C_{11}-C_{44})} .$$

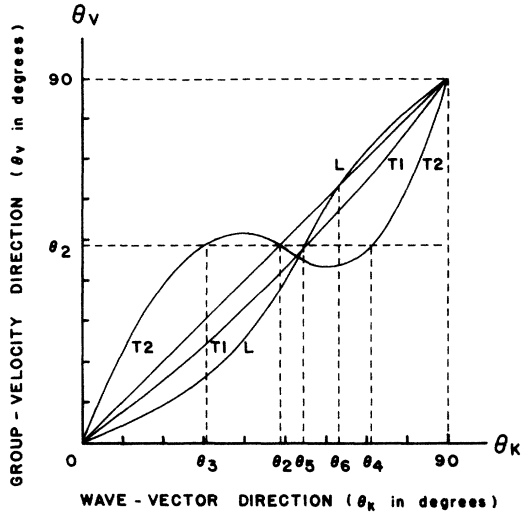

FIG. 1. Relation between the direction of the wave vector and the group-velocity vector for solid helium 4 using the elastic constants of Crepeau *et al.* Angles are measured with respect to the C axis. Note the cuspidal edge in the transverse T_2 mode about θ_2. In the vicinity of the cusp the wave vector is double or triple valued.

The additional collinear point θ_2 for the slow mode is given by[20]

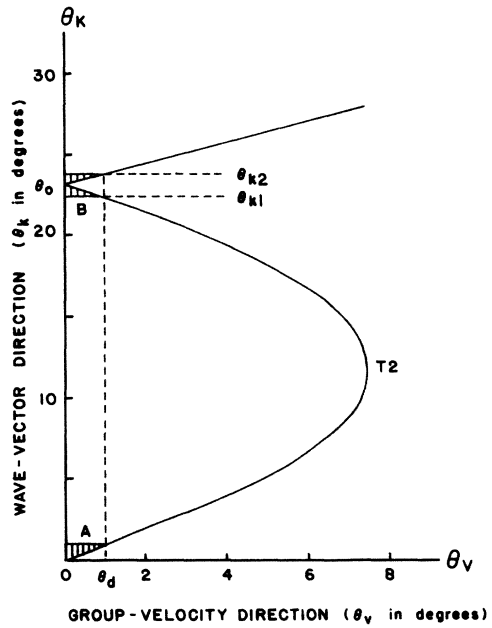

FIG. 2. Relation between the direction of the wave vector and the group velocity vector for apatite which has a cuspidal edge about the C axis. θ_d is the small angle subtended by the phonon detector. In the vicinity $0 < \theta_k < \theta_0$, the wave vector and its corresponding group-velocity vector differ in azimuthal angle ϕ by 180°. The shaded areas indicate the regions of integration for θ_k. The half-width of the cusp is approximately 7.5°.

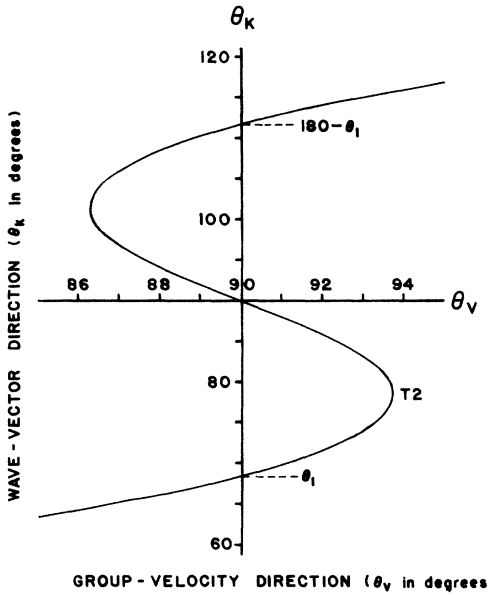

FIG. 3. Relation between the direction of the wave vector and the group-velocity vector for apatite which also has a cuspidal edge about C_L. In the vicinity of the cusp two or three wave vectors can give rise to the same group-velocity vector.

$$\tan\theta_2 = \left(\frac{C_{13}+C_{33}}{C_{13}+C_{11}}\right)^{1/2}, \tag{16}$$

and the additional collinear point θ_6 for the fast mode is

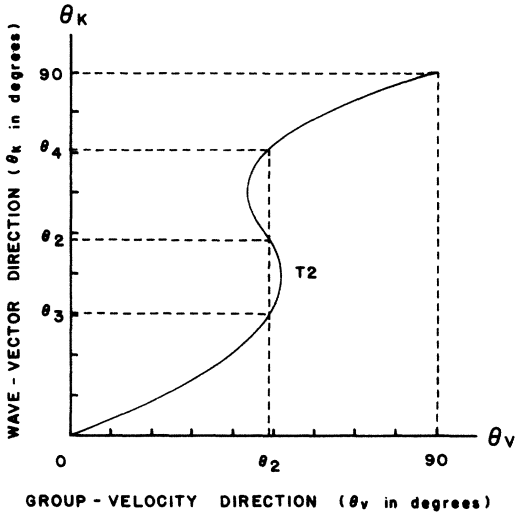

FIG. 4. Relation between the direction of the wave vector and the group-velocity vector for solid helium 4. In the vicinity of the cusp about θ_2 two or three wave vectors can give rise to the same group-velocity vector.

$$\tan\theta_6 = \left(\frac{(C_{13}+C_{44})-(C_{33}-C_{44})}{(C_{13}+C_{44})-(C_{11}-C_{44})}\right)^{1/2}. \quad (17)$$

A solution for the wave-vector directions along which pure modes propagate can be obtained in a similar manner. Results for a number of crystal symmetries have been given by Brugger.[21] Since the wave vector and polarization vector for the fast mode are in the same direction along θ_6, this direction is commonly called the longitudinal axis. Along this same direction the wave vector and polarization vector for the slow mode are perpendicular so this mode propagates as a pure transverse wave. Equation (17) thus gives the additional wave-vector direction along which the corresponding phase and group velocity for the fast mode are parallel and along which pure longitudinal and pure transverse waves propagate.

C. Phonon-amplification factor for cusp-free velocity surfaces

Consider a phonon detector located in the direction (θ_v, ϕ_v) relative to a point source of phonons. The angles (θ_v, ϕ_v) are the spherical polar angles, with θ_v the angle with respect to the C axis. Let the detector as viewed from the source subtend a small solid angle $\Delta\Omega_v$. For a phonon to reach the detector from the source the group velocity must fall within the small solid angle $\Delta\Omega_v$ about the direction (θ_v, ϕ_v). Since the group and phase velocities are, in general, not collinear for an anisotropic solid, let the corresponding solid angle and direction in wave vector or k space be denoted, respectively, by $\Delta\Omega_k$ and (θ_k, ϕ_k). The phonon-amplification factor A is then the ratio of the solid angle in wave vector or k space to the corresponding solid angle in group-velocity space.[8] If cuspidal edges in the group-velocity surface are absent, then the phonon-amplification factor in the direction (θ_v, ϕ_v) for an infinitesimal detector is

$$A(\theta_v, \phi_v) = \frac{d\Omega_k(\theta_k, \phi_k)}{d\Omega_v(\theta_v, \phi_v)} = \frac{d(\cos\theta_k)\,d\phi_k}{d(\cos\theta_v)\,d\phi_v}. \quad (18)$$

Since hexagonal crystals are transversely isotropic, i.e., velocity surfaces are surfaces of revolution about the C axis, this reduces to

$$A(\theta_v) = \frac{\sin\theta_k\, d\theta_k}{\sin\theta_v\, d\theta_v}. \quad (19)$$

Along directions perpendicular to the C axis this becomes

$$A(90^\circ) = \left.\frac{d\theta_k}{d\theta_v}\right|_{\theta_k=\theta_v=90^\circ} \quad (20)$$

and along directions nearly parallel to the C axis

$$A(0^\circ) = \left(\frac{d\theta_k}{d\theta_v}\right)^2_{\theta_k=\theta_v=0^\circ}. \quad (21)$$

The results for each polarization mode are given as follows: Along the C axis,

$$A(0^\circ) = \left[C_{33}\Big/\left(C_{44}+\frac{(C_{13}+C_{44})^2}{(C_{33}-C_{44})}\right)\right]^2, \quad (L \text{ mode}) \quad (22)$$

$$A(0^\circ) = \left(\frac{C_{44}}{C_{66}}\right)^2, \quad (T_1 \text{ mode}) \quad (23)$$

$$A(0^\circ) = \left[C_{44}\Big/\left(C_{11}-\frac{(C_{13}+C_{44})^2}{(C_{33}-C_{44})}\right)\right]^2, (T_2 \text{ mode}); \quad (24)$$

perpendicular to the C axis:

$$A(90^\circ) = C_{11}\Big/\left(C_{44}+\frac{(C_{13}+C_{44})^2}{(C_{11}-C_{44})}\right), \quad (L \text{ mode}) \quad (25)$$

$$A(90^\circ) = \frac{C_{66}}{C_{44}}, \quad (T_1 \text{ mode}) \quad (26)$$

$$A(90^\circ) = C_{44}\Big/\left(C_{33}-\frac{(C_{13}+C_{44})^2}{(C_{11}-C_{44})}\right), \quad (T_2 \text{ mode}). \quad (27)$$

Along the collinear point θ_6 for the fast mode,

$$A(\theta_6) = \left.\frac{d\theta_k}{d\theta_v}\right|_{\theta_k=\theta_v=\theta_6} = \left(1-\frac{4[(C_{13}+C_{44})-(C_{11}-C_{44})][(C_{13}+C_{44})-(C_{13}-C_{44})][(C_{11}-C_{44})(C_{33}-C_{44})-(C_{13}+C_{44})^2]}{\{2(C_{13}+C_{44})-[(C_{11}-C_{44})+(C_{33}-C_{44})]\}(C_{13}+C_{44})[C_{11}C_{33}-(C_{13}+2C_{44})^2]}\right)^{-1} \quad (28)$$

and for the collinear point θ_2 for the slow mode,

$$A(\theta_2) = \left.\frac{d\theta_k}{d\theta_v}\right|_{\theta_k=\theta_v=\theta_2} = \left(1-\frac{4(C_{13}+C_{11})(C_{13}+C_{33})[(C_{11}-C_{44})(C_{33}-C_{44})-(C_{13}+C_{44})^2]}{[(C_{13}+C_{11})+(C_{13}+C_{33})](C_{13}+C_{44})(C_{11}C_{33}-C_{13}^2)}\right)^{-1}. \quad (29)$$

D. Conditions for cuspidal edges

If $d\theta_k/d\theta_v < 0$ a cuspidal edge exists because more than one wave-vector direction with respect to the C axis can give group-velocity vectors along a given direction (see Figs. 1–4). It is readily seen that $d\theta_k/d\theta_v > 0$ for the T_1 mode for all values of θ_v and therefore cuspidal edges are always ab-

sent for this mode.

In considering cuspidal edges in the transverse T_2 and L modes, one must distinguish between several distinct cases. Consider first the case where $C_{33} > C_{44}$ and $C_{11} > C_{44}$, i.e., the fast mode is longitudinal along both C and $C_\perp$. Under these conditions cuspidal edges about C and $C_\perp$ for the fast mode are impossible. The T_2 or slow mode, however, has a cuspidal edge about the C axis if

$$(C_{13}+C_{44})^2 > C_{11}(C_{33}-C_{44}), \quad \text{where } C_{33} > C_{44} \tag{30}$$

or about $C_\perp$ if

$$(C_{13}+C_{44})^2 > C_{33}(C_{11}-C_{44}), \quad \text{where } C_{11} > C_{44}. \tag{31}$$

These conditions have previously been derived by Musgrave by considering the inverse phase velocity surface.[22]

Consider now the case $C_{33} < C_{44}$ for which the fast mode is quasitransverse near the C axis. For this condition no cusp can exist in the fast mode about the C axis. The slow quasilongitudinal mode, however, has a cuspidal edge about the C axis if

$$(C_{13}+C_{44})^2 > C_{44}(C_{44}-C_{33}), \quad \text{where } C_{44} > C_{33} \tag{32}$$

Similarly, if $C_{11} < C_{44}$, the fast mode is quasitransverse near $C_\perp$. Again, no cusp can exist in the fast mode about the $C_\perp$ direction. The slow quasilongitudinal mode, however, has a cuspidal edge about the $C_\perp$ direction, provided

$$(C_{13}+C_{44})^2 > C_{44}(C_{44}-C_{11}), \quad \text{where } C_{44} > C_{11}. \tag{33}$$

Consider now the conditions for cuspidal edges about the collinear points θ_2 and θ_6. For a collinear point θ_2 to exist in the slow mode, Eq. (16) requires $(C_{13}+C_{11})(C_{13}+C_{33}) > 0$, and since $C_{13}+C_{44} > 0$, condition (8) for elastic stability requires $(C_{13}+C_{11}) + (C_{13}+C_{33}) > 0$. Thus from Eq. (29) a cuspidal edge exists in the slow mode at θ_2 if

$$4(C_{13}+C_{11})(C_{13}+C_{33})[(C_{11}-C_{44})(C_{33}-C_{44}) - (C_{13}+C_{44})^2] > [(C_{13}+C_{11})+(C_{13}+C_{33})](C_{13}+C_{44})(C_{11}C_{33}-C_{13}^2). \tag{34}$$

For a collinear point θ_6 to exist in the fast mode, Eq. (17) requires

$$[(C_{13}+C_{44})-(C_{33}-C_{44})][(C_{13}+C_{44})-(C_{11}-C_{44})] > 0. \tag{35}$$

If

$$\{2(C_{13}+C_{44})-[(C_{11}-C_{44})+(C_{33}-C_{44})]\}(C_{14}+C_{44})[C_{11}C_{33}-(C_{13}+2C_{44})^2] > 0$$

in Eq. (28), then a cuspidal edge exists in the fast mode about θ_6 if

$$4[(C_{13}+C_{44})-(C_{11}-C_{44})][(C_{13}+C_{44})-(C_{33}-C_{44})][(C_{11}-C_{44})(C_{33}-C_{44})-(C_{13}+C_{44})^2]$$
$$> \{2(C_{13}+C_{44})-[(C_{11}-C_{44})+(C_{33}-C_{44})]\}(C_{13}+C_{44})[C_{11}C_{33}-(C_{13}+2C_{44})^2]. \tag{36}$$

This cannot be satisfied unless

$$(C_{11}-C_{44})(C_{33}-C_{44}) > (C_{13}+C_{44})^2. \tag{37}$$

Furthermore, since a cuspidal edge at θ_6 requires defocusing of the fast mode about C and $C_\perp$ (see Sec. II E) and this is inconsistent with inequality (37), inequality (36) cannot be satisfied. If, however,

$$\{2(C_{13}+C_{44})-[(C_{11}-C_{44})+(C_{33}-C_{44})]\}(C_{13}+C_{44})[C_{11}C_{33}-(C_{13}+2C_{44})^2] < 0, \tag{38}$$

then a cuspidal edge exists in the fast mode about θ_6 if

$$4[(C_{13}+C_{44})-(C_{11}-C_{44})][(C_{13}+C_{44})-(C_{33}-C_{44})][(C_{13}+C_{44})^2-(C_{11}-C_{44})(C_{33}-C_{44})]$$
$$> \{2(C_{13}+C_{44})-[(C_{11}-C_{44})+(C_{33}-C_{44})]\}(C_{13}+C_{44})[(C_{13}+2C_{44})^2-C_{11}C_{33}]. \tag{39}$$

Again, to satisfy this inequality

$$(C_{13}+C_{44})^2 > (C_{11}-C_{44})(C_{33}-C_{44}), \tag{40}$$

and this is now consistent with the requirement that defocusing of the fast mode occur about C and $C_\perp$ (see Sec. II E). Thus for $C_{13}+C_{44} > 0$, inequalities (35) and (40) require

$$2(C_{13}+C_{44})-[(C_{11}-C_{44})+(C_{33}-C_{44})] > 0.$$

With inequality (38) this requires

$$(C_{13}+2C_{44})^2 - C_{11}C_{33} > 0$$

This inequality can be rewritten as

$$4C_{44}(C_{13}+C_{44}) > C_{11}C_{33} - C_{13}^2$$

and using the elastic stability condition (8) gives

$$(C_{13}+C_{44}) > C_{33}C_{66}/4C_{44} > 0.$$

TABLE I. Elastic constants of some hexagonal crystals. The elastic constants of helium 4 are multiplied by 10^8; all others are multiplied by 10^{11} for units of dyn/cm^2. The values listed at 0°K have been extrapolated by the authors from measurements performed at liquid-helium temperatures. For ice and D_2O, however, the values at 0°K were obtained by evaluating curve-fitted polynomials to data measured down to −140°C.

Material	Elastic constants C_{11}	C_{33}	C_{44}	C_{66}	C_{13}	T(°K)
Apatite[a]	16.67	13.96	6.63	7.68	6.55	R.T.
Beryl[b]	28.73	24.18	7.02	9.41	7.29	R.T.
Beryllium[c]	29.94	34.22	16.62	13.59	1.1	0
Beryllium oxide[d]	46.06	49.16	14.77	16.70	8.848	298
Cadmium[e]	13.08	5.737	2.449	4.516	4.145	0
Cadmium selenide[d]	7.490	8.451	1.315	1.441	3.926	298
Cadmium sulfide[f]	8.76	9.58	1.48	1.65	4.825	0
Calcium magneside[g]	6.124	6.552	1.927	2.183	1.5	100
Cobalt[h]	30.71	35.81	7.55	7.105	10.27	298
Hafnium[i]	19.01	20.44	6.00	5.78	6.55	4
Helium 4[j]	4.66	6.05	1.84	1.02	0.23	
Helium 4[k]	5.50	7.10	1.40	1.30	1.31	
Helium 4[l]	4.04	5.53	1.21	0.963	1.05	
Ice[m]	1.2904	1.4075	0.2819	0.32085	0.5622	0
Ice (D_2O)[n]	1.6992	2.0247	0.4276	0.4134	0.5904	0
Magnesium[o]	6.348	6.645	1.842	1.875	2.17	0
Rhenium[p]	63.44	70.16	16.91	18.41	20.2	4.2
Thallium[q]	4.44	6.02	0.880	0.341	3.0	4.2
Titanium[i]	17.61	19.05	5.08	4.46	6.83	4
Yttrium[r]	8.34	8.01	2.715	2.690	1.9	0
Zinc[s]	17.696	6.848	4.589	7.108	5.279	0
Zinc[t]	17.909	6.880	4.595	7.080	5.54	4.2
Zinc oxide[u]	20.97	21.09	4.247	4.429	10.51	298
Zinc sulfide[v]	13.12	14.08	2.86	3.245	5.09	R.T.
Zinc sulfide[d]	12.42	14.00	2.864	3.203	4.554	298
Zinc sulfide[w]	12.40	14.04	2.85	3.20	4.5	R.T.
Zirconium[i]	15.54	17.25	3.63	4.41	6.46	4

[a]J. Bhimasenachar, Proc. Indian Acad. Sci. A 22, 209 (1945).
[b]B. Ramachandra Rao, Proc. Indian Acad. Sci. A 22, 194 (1945).
[c]J. F. Smith and C. L. Arbogast, J. Appl. Phys. 31, 99 (1960).
[d]C. F. Cline, H. L. Dunegan, and G. W. Henderson, J. Appl. Phys. 38, 1944 (1967).
[e]C. W. Garland and J. Silverman, Phys. Rev. 119, 1218 (1960).
[f]D. Gerlich, J. Phys. Chem. Solids 28, 2575 (1967).
[g]Ali Sumer and J. F. Smith, J. Appl. Phys. 33, 2283 (1962).
[h]H. J. McSkimin, J. Appl. Phys. 26, 406 (1955).
[i]E. S. Fisher and C. J. Renken, Phys. Rev. 135, A482 (1964).
[j]D. S. Greywall, Phys. Rev. A 3, 2106 (1971). These constants were measured at a molar volume of 20.5 cm^3.
[k]J. P. Franck and R. Wanner, Phys. Rev. Lett. 25, 345 (1970). These constants were measured at a molar volume of 20.32 cm^3.
[l]R. H. Crepeau, O. Heybey, D. M. Lee, and S. A. Strauss, Phys. Rev. A 3, 1162 (1971). These constants were measured at a molar volume of 20.97 cm^3.
[m]G. Dantl, Phys. Kondens. Mater. 7, 390 (1968).
[n]U. Mitzdorf and D. Helmreich, J. Acoust. Soc. Am. 49, 723 (1971).
[o]L. J. Slutsky and C. W. Garland, Phys. Rev. 107, 972 (1957).
[p]M. L. Shepard and J. F. Smith, J. Appl. Phys. 36, 1447 (1965).
[q]R. W. Ferris, M. L. Shepard and J. F. Smith, J. Appl. Phys. 34, 768 (1963).
[r]J. F. Smith and J. A. Gjevre, J. Appl. Phys. 31, 645 (1960). Shepard and Smith (footnote p) report that the elastic constants C_{44} and C_{66} for yttrium were mistakenly interchanged.
[s]C. W. Garland and R. Dalven, Phys. Rev. 111, 1232 (1958).
[t]G. A. Alers and J. R. Neighbours, J. Phys. Chem. Solids 7, 58 (1958).
[u]T. B. Bateman, J. Appl. Phys. 33, 3309 (1962).
[v]J. DeKlerk, J. Phys. Chem. Solids 28, 1831 (1967).
[w]V. G. Zubov, L. A. Sysoev, and M. M. Firsova, Kristallografiya 12, 84 (1967) [Sov. Phys.-Crystallogr. 12, 67 (1967)].

A cusp, if it exists, will most likely occur when

$$(C_{13}+C_{44}) \gg |C_{11}-C_{44}|, \quad (C_{13}+C_{44}) \gg |C_{33}-C_{44}| .$$

This is equivalent to the conditions

$$C_{11} \simeq C_{44}, \quad C_{33} \simeq C_{44}, \quad C_{13} \lesssim C_{44} .$$

On expanding inequality (39) in powers of $(C_{13}+C_{44})$ it is readily seen that there are no conditions consistent with elastic stability for which this inequality can be satisfied. As a result cuspidal edges cannot occur in the fast mode about the collinear point θ_6. Since cuspidal edges in the group-velocity surface for the fast mode and the T_1 mode are not possible, they can occur only for the slow mode.

If a cuspidal edge occurs in the slow mode about C axis then wave vectors at angle θ_0 give group-velocity vectors parallel to the C axis where θ_0 is given by

$$\tan^2\theta_0 = -\left(\frac{2(C_{13}+C_{44})^2-(C_{11}-C_{44})(C_{33}-C_{44})}{(C_{11}-C_{44})^2}\right) + \frac{(C_{11}+C_{44})(C_{13}+C_{44})}{(C_{11}-C_{44})^2} \times \left(\frac{(C_{13}+C_{44})^2-(C_{11}-C_{44})(C_{33}-C_{44})}{C_{11}C_{44}}\right)^{1/2} \tag{41}$$

Similarly a cuspidal edge about $C_\perp$ gives wave vectors at angle θ_1 with group-velocity vectors along $C_\perp$, where $\cot^2\theta_1$ replaces $\tan^2\theta_0$, C_{11} replaces C_{33}, and C_{33} replaces C_{11} in Eq. (41).

If, however, a cuspidal edge occurs about the collinear point $\theta_k=\theta_v=\theta_2$, for example, solving for the other values of θ_k giving $\theta_v=\theta_2$ results in a sixth-degree equation in $\tan\theta_k$. This equation is identical for the fast and slow modes. Although one root, $\tan\theta_2$, can be extracted, the resulting equation—being of fifth degree—has no general algebraic solution and one of the remaining roots must be determined numerically. It is most convenient to determine numerically a root, $\tan\theta_5$, corresponding to $\theta_v=\theta_2$ for the fast mode. The resulting quartic equation can be factored using the method of Descartes or Ferrari,[23] giving a pair of positive real roots $\tan\theta_3$, $\tan\theta_4$, respectively, and a pair of complex conjugate roots. Such a solution has been performed for a number of hexagonal crystals and the results are listed in Table II.

E. Conditions for phonon focusing at collinear cusp-free points

Phonon focusing is said to occur if $A(\theta_v)>1$. For collinear cusp-free points this is equivalent to

$$\left.\frac{d\theta_k}{d\theta_v}\right|_{\theta_k=\theta_v} > 1 .$$

Thus for cusp-free focusing to occur along the C axis

$$(C_{33}-C_{44})^2 > (C_{13}+C_{44})^2, \quad \text{if } C_{33}>C_{44} \qquad \text{(fast } L \text{ mode)} \tag{42}$$

but

$$(C_{44}-C_{33})^2 < (C_{13}+C_{44})^2 < C_{44}(C_{44}-C_{33}) \quad \text{if } C_{44}>C_{33} \qquad \text{(slow } L \text{ mode)}; \tag{43}$$

$$C_{44}>C_{66}, \qquad (T_1 \text{ mode}) \tag{44}$$

$$C_{11}(C_{33}-C_{44}) > (C_{13}+C_{14})^2 > (C_{11}-C_{44})(C_{33}-C_{44}) \quad \text{if } C_{33}>C_{44}, \qquad \text{(slow } T_2 \text{ mode)} \tag{45}$$

but

$$(C_{13}+C_{44})^2 < (C_{11}-C_{44})(C_{33}-C_{44}) \quad \text{if } C_{44}>C_{33} \qquad \text{(fast } T_2 \text{ mode)}. \tag{46}$$

Inequality (46) is valid only if $C_{44}>C_{33}$ and $C_{44}>C_{11}$.

Similarly, for cusp-free phonon focusing to occur along $C_\perp$

$$(C_{11}-C_{44})^2 > (C_{13}+C_{44})^2 \quad \text{if } C_{11}>C_{44} \qquad \text{(fast } L \text{ mode)} \tag{47}$$

but

$$(C_{44}-C_{11})^2 < (C_{13}+C_{44})^2 < C_{44}(C_{44}-C_{11}) \quad \text{if } C_{44}>C_{11} \qquad \text{(slow } L \text{ mode)}; \tag{48}$$

$$C_{66}>C_{44}, \qquad (T_1 \text{ mode}) \tag{49}$$

$$C_{33}(C_{11}-C_{44}) > (C_{13}+C_{44})^2 > (C_{11}-C_{44})(C_{33}-C_{44}) \quad \text{if } C_{11}>C_{44}, \qquad \text{(slow } T_2 \text{ mode)} \tag{50}$$

but

$$(C_{13}+C_{44})^2 < (C_{11}-C_{44})(C_{33}-C_{44}) \quad \text{if } C_{44}>C_{11} \qquad \text{(fast } T_2 \text{ mode)}. \tag{51}$$

Again, inequality (51) is valid only if $C_{44} > C_{11}$ and $C_{44} > C_{33}$.

For focusing of the slow mode along the collinear point θ_2,

$$(C_{13}+C_{44})^2 < (C_{11}-C_{44})(C_{33}-C_{44}) \quad \text{if } (C_{11}-C_{44})(C_{33}-C_{44}) > 0. \tag{52}$$

and no cusp is present about θ_2.

Finally, for focusing of the fast mode along the collinear point θ_6,

$$(C_{13}+C_{44})^2 > (C_{11}-C_{44})(C_{33}-C_{44}). \tag{53}$$

F. Phonon-amplification factor in the presence of cuspidal edges

The presence of cuspidal edges increases the amplification factor because more than one wave vector contributes to a given group-velocity vector. For a cusp about the C axis it is necessary to consider a finite angle θ_d subtending the C axis, and integrate over all phonon wave vectors that give rise to phonon group velocities within this solid angle. Because of the finite size of phonon bolometers, θ_d can be expected to be of the order of 1°. The angle θ_d must be small compared to the half-width of the cusp for the following approximations to be valid.[24] The contribution to the integral over wave vectors from region A (see Fig. 2) is given by

$$\Delta\Omega_k = -2\pi \int_0^{\Delta\theta_k} \sin\theta_k \, d\theta_k \simeq -2\pi \frac{(\Delta\theta_k)^2}{2},$$

where θ_k replaces $\sin\theta_k$ for small angles.

Since

$$\Delta\theta_k \simeq \frac{d\theta_k}{d\theta_v}\Delta\theta_v = \frac{d\theta_k}{a\theta_v}\theta_d,$$

thus

$$\Delta\Omega_k = -2\pi\left(\frac{d\theta_k}{d\theta_v}\right)^2_{\theta_k=0}\frac{\theta_d^2}{2}.$$

The contribution from region B is

$$\Delta\Omega_k = -2\pi \int_{\theta_{k1}}^{\theta_{k2}} \sin\theta_k \, d\theta_k \simeq -2\pi \int_{\theta_0}^{\theta_{k2}} 2\sin\theta_k \, d\theta_k$$

TABLE II. Collinear points and cuspidal edges in some hexagonal crystals. Symbols are defined in the text. The angles θ are measured in degrees. Entries under θ_0 and θ_1 indicate cuspidal edges about directions parallel to and perpendicular to the C axis, respectively. Entries under θ_3 and θ_4 indicate cuspidal edges about directions having an angle θ_2 with respect to the C axis.

Material	θ_0	θ_1	θ_2	θ_3	θ_4	θ_5	θ_6
Apatite	23.16	68.41	43.22	...	...	...	53.77
Beryl	...	...	43.07	27.10	55.51	39.44	31.82
Beryllium	...	...	46.85	...	...	...	9.38
Beryllium oxide	...	...	45.79	35.96	57.15	47.15	49.84
Cadmium	4.87	...	37.14	...	...	...	...
Cadmium selenide	...	...	46.16	24.00	69.76	48.79	54.93
Cadmium sulfide	...	...	45.84	26.29	66.70	47.87	53.61
Calcium magneside	...	...	45.78	...	...	...	51.28
Cobalt	...	...	46.68	25.48	69.84	49.69	54.43
Hafnium	...	...	45.78	...	...	...	63.74
Helium 4	...	...	48.59	34.66	67.36	53.22	59.27
Helium 4	...	...	48.02	21.46	76.03	52.07	55.71
Helium 4	...	...	48.66	30.57	71.24	54.48	63.21
Ice (H_2O)	...	...	45.88	30.28	63.07	47.80	52.61
Ice (D_2O)	...	...	46.90	27.38	68.92	50.42	56.51
Magnesium	...	...	45.49	...	...	...	51.68
Rhenium	...	...	46.11	31.51	62.66	48.24	52.62
Thallium	...	...	47.75	...	...	...	...
Titanium	...	...	45.82	...	...	...	61.25
Yttrium	...	...	44.53	...	...	...	39.37
Zinc	24.52	71.23	36.00	...	...	...	...
Zinc	25.06	67.94	36.05	...	...	...	...
Zinc oxide	...	...	45.05	...	...	...	45.85
Zinc sulfide	...	...	45.74	24.97	67.47	47.20	49.95
Zinc sulfide	...	...	46.27	25.10	69.01	48.69	52.83
Zinc sulfide	...	...	46.33	24.53	69.66	48.80	52.88
Zirconium	...	...	46.07	32.76	61.46	48.39	54.32

$$= -2\pi(2\sin\theta_0)\Delta\theta_k$$

or

$$\Delta\Omega_k = -4\pi\sin\theta_0\frac{d\theta_k}{d\theta_v}\theta_d,$$

where

$$\theta_0 = \frac{\theta_{k1}+\theta_{k2}}{2},$$

$$\Delta\theta_k = \frac{\theta_{k2}-\theta_{k1}}{2} \simeq \frac{d\theta_k}{d\theta_v}\Delta\theta_v = \frac{d\theta_k}{d\theta_v}\theta_d.$$

The total contribution from regions A and B is

$$\Delta\Omega_k = -2\pi\left(\frac{d\theta_k}{d\theta_v}\right)^2_{\theta_k=\theta_v=0}\frac{\theta_d^2}{2} - 4\pi\sin\theta_0\frac{d\theta_k}{d\theta_v}\theta_d. \quad (54)$$

The integral over the group velocities is just

$$\Delta\Omega_v = -2\pi\int_0^{\theta_d}\sin\theta_v d\theta_v \simeq -2\pi\frac{\theta_d^2}{2}. \quad (55)$$

The phonon amplification for the solid angle θ_d about the C axis is

$$A = \frac{\Delta\Omega_k}{\Delta\Omega_v} = \left(\frac{d\theta_k}{d\theta_v}\right)^2_{\theta_k=\theta_v=0} + \frac{4\sin\theta_0}{\theta_d}\left(\frac{d\theta_k}{d\theta_v}\right)_{\theta_k=\theta_0,\,\theta_v=0}, \quad (56)$$

where

$$\left(\frac{d\theta_k}{d\theta_v}\right)_{\theta_k=\theta_0} = \frac{(y/z)}{2\tan^2\theta_0}, \quad (57)$$

$$y = (C_{33}+C_{44})(C_{13}+C_{44})\left(\frac{(C_{13}+C_{44})^2-(C_{11}-C_{44})(C_{33}-C_{44})}{C_{11}C_{44}}\right)^{1/2}$$
$$-\{(C_{33}-C_{44})^2+\tan^2\theta_0[2(C_{13}+C_{44})^2-(C_{11}-C_{44})(C_{33}-C_{44})]\}, \quad (58)$$

$$z = 2(C_{13}+C_{44})^2-(C_{11}-C_{44})(C_{11}-C_{44}+C_{33}-C_{44})$$
$$+\frac{(C_{11}+C_{44})[2(C_{13}+C_{44})^2-(C_{33}-C_{44})(C_{11}-C_{44}+C_{33}-C_{44})-(w)\tan^2\theta_0]}{(C_{13}+C_{44})\{[(C_{13}+C_{44})^2-(C_{11}-C_{44})(C_{33}-C_{44})]/C_{11}C_{44}\}^{1/2}}, \quad (59)$$

TABLE III. The phonon-amplification factor in hexagonal crystals at collinear points. For elastically isotropic solids the amplification factor $A(\theta_v)$ is unity. The angle θ_d subtended by a detector along the C axis was chosen to be 1° for solids having cuspidal edges about the C axis. The calculations for all other cases correspond to those for an infinitesimal detector.

Material	$A(0°)$ L	T_1	T_2	$A(90°)$ L	T_1	T_2	$A(\theta_6)$ L	$A(\theta_2)$ T_2
Apatite	0.212	0.745	73.60	0.697	1.158	4.419	1.636	0.365
Beryl	1.628	0.557	0.175	1.746	1.340	0.476	0.713	9.428
Beryllium	0.986	1.496	1.887	0.745	0.818	1.561	1.014	0.775
Beryllium oxide	2.516	0.782	0.245	1.413	1.131	0.471	0.668	15.71
Cadmium	0.134	0.294	76.30	2.000	1.844	1.487	···	0.640
Cadmium selenide	2.678	0.833	0.130	1.300	1.096	0.329	0.719	3.741
Cadmium sulfide	2.249	0.805	0.148	1.262	1.115	0.359	0.752	5.182
Calcium magneside	2.152	0.779	0.289	1.296	1.133	0.513	0.732	13.38
Cobalt	3.633	1.129	0.150	1.444	0.941	0.342	0.631	3.466
Hafnium	1.462	1.078	0.548	1.050	0.963	0.720	0.925	1.581
Helium 4	4.494	3.213	0.254	1.391	0.558	0.405	0.611	5.228
Helium 4	6.975	1.160	0.111	1.723	0.929	0.264	0.497	1.815
Helium 4	5.025	1.667	0.195	1.297	0.775	0.340	0.673	3.834
Ice (H_2O)	2.367	0.772	0.184	1.306	1.138	0.402	0.725	7.657
Ice (D_2O)	3.538	1.070	0.166	1.367	0.967	0.353	0.662	4.075
Magnesium	1.637	0.965	0.378	1.172	1.018	0.599	0.825	2.772
Rhenium	2.691	0.834	0.202	1.364	1.089	0.417	0.685	7.762
Thallium	2.498	6.660	0.339	0.869	0.388	0.491	···	4.331
Titanium	1.564	1.297	0.464	1.074	0.878	0.657	0.898	1.943
Yttrium	1.413	1.019	0.395	1.283	0.991	0.643	0.814	2.416
Zinc	0.021	0.417	37.10	1.472	1.549	15.62	···	0.300
Zinc	0.019	0.421	36.28	1.455	1.541	10.83	···	0.285
Zinc oxide	1.508	0.920	0.279	1.214	1.043	0.526	0.822	5.656
Zinc sulfide	2.748	0.777	0.146	1.455	1.135	0.361	0.657	4.106
Zinc sulfide	3.217	0.800	0.147	1.440	1.118	0.348	0.644	3.684
Zinc sulfide	3.344	0.793	0.142	1.458	1.123	0.340	0.635	3.432
Zirconium	2.413	0.678	0.203	1.276	1.215	0.417	0.735	10.05

$$w = 2(C_{13}+C_{44})^2 - (C_{11}-C_{44})(C_{11}-C_{44}+C_{33}-C_{44}), \tag{60}$$

and $\tan^2\theta_0$ is given by Eq. (41).

For a cusp about $C_\perp$ the phonon-amplification factor is straightforward to derive. The result is

$$A = \left|\frac{d\theta_k}{d\theta_v}\right|_{\theta_k=\theta_v=90^\circ} + 2\sin\theta_1 \left.\frac{d\theta_k}{d\theta_v}\right|_{\theta_k=\theta_1,\,\theta_v=90^\circ}, \tag{61}$$

where

$$\left|\frac{d\theta_k}{d\theta_v}\right|_{\theta_k=\theta_1,\,\theta_v=90^\circ}$$

is given by Eqs. (57)–(60) but with $\cot^2\theta_1$ replacing $\tan^2\theta_0$, C_{33} replacing C_{11} and C_{11} replacing C_{33}.

For a cusp about the collinear point θ_2 the derivation is quite similar. The result is

$$A = \left|\frac{d\theta_k}{d\theta_v}\right|_{\theta_k=\theta_v=\theta_2} + \frac{\sin\theta_3}{\sin\theta_2}\left.\frac{d\theta_k}{d\theta_v}\right|_{\theta_k=\theta_3,\,\theta_v=\theta_2} + \frac{\sin\theta_4}{\sin\theta_2}\left.\frac{d\theta_k}{d\theta_v}\right|_{\theta_k=\theta_4,\,\theta_v=\theta_2}, \tag{62}$$

and $d\theta_k/d\theta_v|_{\theta_k=\theta_v=\theta_2}$ is given by Eq. (29). The value of $d\theta_k/d\theta_v$ at impure-mode points $\theta_k=\theta_3$, θ_4 can be determined numerically. Calculation of the phonon-amplification factor at all collinear points are listed in Table III.

To determine the phonon-amplification factor at other directions it is most convenient to use numerical integration to count the number of group-velocity vectors falling within a small solid angle for a uniform angular density of k vectors. This has been done for a number of hexagonal crystals. The results are tabulated in Table IV for helium 4.

G. Effect of phonon focusing on phonon conduction

Since in hexagonal crystals the phonon phase velocity for each mode along directions parallel and perpendicular to the C axis are different, the thermal conductivity is expected to be anisotropic at all temperatures. In the boundary-scattering regime (i.e., ballistic phonon propagation), however, focusing can be responsible for anisotropic heat conduction even when the phonon phase velocities along directions parallel and perpendicular to the C axis are equal. Focusing will always be present whenever a solid is elastically anisotropic and occurs even in cubic crystals.

To illustrate the effects of focusing, therefore, calculations were performed to determine the phonon-conduction-enhancement factor A_κ, defined as

$$A_\kappa = \kappa_v/\kappa_s, \tag{63}$$

where κ_v is the thermal conductivity calculated by correctly including the effects of phonon focusing and κ_s is the thermal conductivity calculated using phase-velocity vectors instead of group-velocity vectors in each mode. Calculations of κ_s thus disregard the angular deviation between the group-velocity vectors and their corresponding wave vectors for elastically anisotropic solids. Values of κ_s will depend upon the orientation of the rod axis and will be largest for directions coinciding with the largest inverse-square phase velocity averaged over the three modes.

Calculations of κ_v and κ_s were performed for samples of circular cross section with a length-to-diameter ratio of 10. It must be emphasized that this length is not the geometric length of the crystal but a thermal length and is measured along the sample rod axis between the centers of the heat source and heat sink, respectively.[7,9] Calculations of the Casimir velocity v_c and the lattice specific heat C_v/T^3 for five solids are listed in Table V. The Casimir velocity is defined as

$$v_c = \langle s^{-2}\rangle/\langle s^{-3}\rangle, \tag{64}$$

where $\langle s^{-2}\rangle$ and $\langle s^{-3}\rangle$ are, respectively, averages of the inverse square and inverse cube of the phonon phase velocity for the three modes over all directions. Calculations of the thermal conductivity κ/T^3, the effective phonon mean free path $\Lambda_{\rm corr}$, and the thermal-conduction-enhancement factor A_κ, as a function of the heat-flow direction with respect to the C axis are given in Table VI. The thermal conductivity κ was calculated using the theory of McCurdy, Maris, and Elbaum.[7,9] The

TABLE IV. Calculated intensities of phonons in solid helium 4 as a function of the angle θ with respect to the C axis. A uniform density of wave vectors is assumed. The corresponding intensities for an elastically isotropic solid are unity. Calculations were performed using the elastic constants of R. H. Crepeau, O. Heybey, D. M. Lee, and S. A. Strauss [Phys. Rev. A 3, 1162 (1971)] at a molar volume of 20.97 cm^3.

θ (deg)	L	T_1	T_2	θ (deg)	L	T_1	T_2
0	4.9	1.4	0.2	46	0.7	1.1	4.0
2	4.8	1.6	0.2	48	0.5	1.0	4.0
4	4.8	1.7	0.2	50	0.6	1.1	4.5
6	4.3	1.7	0.2	52	0.6	1.0	4.1
8	4.0	1.7	0.2	54	0.5	1.0	0.8
10	3.4	1.5	0.2	56	0.6	0.9	0.6
12	3.1	1.6	0.2	58	0.6	1.0	0.7
14	2.8	1.5	0.2	60	0.7	0.9	0.6
16	2.3	1.6	0.2	62	0.6	0.8	0.4
18	1.9	1.5	0.2	64	0.7	0.9	0.5
20	1.8	1.5	0.2	66	0.7	0.8	0.4
22	1.6	1.5	0.2	68	0.8	0.8	0.4
24	1.4	1.3	0.2	70	0.8	0.8	0.4
26	1.2	1.5	0.2	72	0.9	0.8	0.4
28	1.1	1.3	0.3	74	0.9	0.8	0.4
30	1.0	1.3	0.3	76	1.0	0.8	0.3
32	0.9	1.3	0.3	78	1.0	0.8	0.4
34	0.9	1.3	0.4	80	1.1	0.8	0.4
36	0.7	1.2	0.4	82	1.2	0.8	0.3
38	0.7	1.2	0.4	84	1.2	0.8	0.3
40	0.7	1.1	0.5	86	1.3	0.7	0.4
42	0.6	1.1	0.5	88	1.3	0.8	0.3
44	0.7	1.1	8.5	90	1.2	0.8	0.4

TABLE V. Casimir velocity v_c and lattice specific heat C_v/T^3 for selected hexagonal crystals at very low temperatures. All densities and elastic constants are low-temperature values. Elastic constants of helium 4 are multiplied by 10^8; all others are multiplied by 10^{10} for units of dyn/cm^2. The density of cadmium was calculated from the value[a] of 8.7491 gm/cm^3 at 25°C obtained from x-ray data[b] and the linear coefficients of thermal expansion.[c] For thallium, the density was calculated from the room temperature value[d] of 11.56 gm/cm^3 derived from x-ray data and the fractional change in volume.[e] The room temperature value[f] of 7.134 gm/cm^3 obtained from x-ray data[g] and the fractional change in volume[e] were used to calculate the low-temperature density of zinc. The density of zirconium, however, was calculated directly from the measured lattice parameters[h] at 4.2°K.

Material	Density (gm cm^{-3})	Elastic constants C_{11}	C_{33}	C_{44}	C_{66}	C_{13}	v_c (km sec^{-1})	C_v/T^3 (erg deg^{-4} cm^{-3})
Cadmium	8.9078	130.8[a]	57.37	24.49	45.16	41.45	1.844	158.0
Helium 4	4.0/20.97	4.04[i]	5.53	1.21	0.963	1.05	0.2670	53730
Thallium	11.81	44.4[c]	60.2	8.80	3.41	30.0	0.7193	2221
Zinc	7.275	176.96[j]	68.48	45.89	71.08	52.79	2.529	60.79
Zirconium	6.5202	155.4[k]	172.5	36.3	44.1	64.6	2.686	53.45

[a]C. W. Garland and J. Silverman, Phys. Rev. 119, 1218 (1960).
[b]E. R. Jette and F. Foote, J. Chem. Phys. 3, 605 (1935).
[c]R. D. McCammon and G. K. White, Philos. Mag. 11, 1125 (1965).
[d]R. W. Ferris, M. L. Shepard and J. F. Smith, J. Appl. Phys. 34, 768 (1963).
[e]R. W. Meyerhoff and J. F. Smith, J. Appl. Phys. 33, 219 (1962).
[f]G. A. Alers and J. R. Neighbours, J. Phys. Chem. Solids 7, 58 (1958).
[g]H. E. Swanson and E. Tatge, Circ. U. S. Natl. Bur. Stand. 1, 16 (1953).
[h]J. Goldak, L. T. Lloyd, and C. S. Barrett, Phys. Rev. 144, 478 (1966).
[i]R. H. Crepeau, O. Heybey, D. M. Lee, and S. A. Strauss, Phys. Rev. A 3, 1162 (1971).
[j]C. W. Garland and R. Dalven, Phys. Rev. 111, 1232 (1958).
[k]E. S. Fisher and C. J. Renken, Phys. Rev. 135, A482 (1964).

diameter of the solid-helium-4 sample was 1.773 mm, the value used in the thermal-conductivity experiments of Hogan, Guyer, and Fairbank.[25] The remaining samples had a diameter of 3 mm. The effective phonon mean free path Λ_{corr} was calculated using the relation

$$\kappa = \tfrac{1}{3} C_v v_c \Lambda_{corr} . \tag{65}$$

For elastically isotropic solids the thermal-conduction-enhancement factor A_κ is unity and the effective phonon mean free path is equal to the Casimir length Λ_c. The Casimir length end corrected for samples with a thermal length 10 times the rod diameter D is

$$\Lambda_c = 0.926D . \tag{66}$$

For dielectric solids (helium 4) these results should be applicable at temperatures which are a small fraction of the Debye temperature. For superconductors, however, (cadmium, thallium, zinc, and zirconium) these results will not be applicable until the temperature becomes a small fraction of the superconducting transition temperature.

III. DISCUSSION

The presence of cuspidal edges has been previously reported in beryl and zinc[13] and more recently in zinc sulfide.[26] It is interesting to note that cusps about directions parallel and perpendicular to the C axis are relatively rare, but cusps about the collinear point θ_2 are common, occurring in approximately half of the solids listed. Since all solids listed have a $C_{13} > 0$, they have a collinear point θ_2 and as a result focusing occurring in the T_2 mode about this point must be accompanied by defocusing for this mode both parallel and perpendicular to the C axis. Furthermore, a cuspidal edge about either C or $C_\perp$, or the presence of focusing about these directions must be accompanied by defocusing of the T_2 mode about θ_2. Three solids listed do not have a collinear point θ_6 because focusing (defocusing) does not occur for the L mode both parallel and perpendicular to the C axis. If, however, focusing occurs in the L mode about θ_6, it must be accompanied by defocusing in the T_2 mode about θ_2. Similarly, if defocusing occurs in the L mode about θ_6, it must be accompanied by focusing about θ_2 or the presence of a cuspidal edge about θ_2 in the T_2 mode. It is also evident that focusing (defocusing) occurring in the T_1 mode about the C axis must result in defocusing (focusing) for this mode about $C_\perp$.

Note that the presence of cuspidal edges give rise to a large phonon-amplification factor. The amount of enhancement is related to the width of the cusp (the narrower the cusp the higher the phonon intensity) and to the angle the cusp of revolution makes with the C axis. It is easy to see that since the velocity surfaces are surfaces of revolu-

tion about the C axis, the presence of phonon focusing or of cuspidal edges about this axis gives rise to the highest intensities. A very narrow cusp about $C_\perp$, however, can still give a large phonon-amplification factor, as illustrated by zinc, but the highest intensities will occur for cuspidal edges about the C axis (e.g., zinc, apatite, and cadmium). In the case of cadmium the width of the cusp is less than 0.25°, giving an extremely high-intensity small-diameter beam of phonons along the C axis. One can also have a large phonon-amplification factor in the absence of a cusp provided the group-velocity vector varies very slowly with wave vector. A case in point is calcium magneside ($CaMg_2$) about the point θ_2, where conditions for a cuspidal edge are nearly satisfied.

Heat-pulse experiments were recently reported[27] in solid helium 4. Listed in Table IV are calculations of the phonon intensity as a function of the angle to the C axis in helium 4 for a uniform density of wave vectors. The results were calculated using numerical integration to count the number of group-velocity vectors falling within 2° intervals for a uniform density of k vectors. For a sufficiently fine mesh in k space, the results should agree along collinear points with the results in Table III. Note that along directions parallel and perpendicular to the C axis the intensities of longitudinal and transverse-T_1 waves are much stronger than the T_2 wave. To observe strong T_2 waves one should look in the vicinity of the cusp center, approximately 48° to the C axis. Still-higher intensities occur along the cusp's edges.

Since the phonon conductivity at very low temperatures is approximately inversely proportional to the square of the phonon velocity, the transverse modes, because of their lower velocity, contribute most to the flow of heat. Energy flow in such a solid should be enhanced along those crystallographic directions where these modes are strongly focused. Cuspidal edges associated with strong focusing are always absent for the transverse T_1

TABLE VI. Summary of theoretical results for selected hexagonal crystals at very low temperatures. Calculations were performed for samples in the form of circular cross-section rods with a thermal length of ten rod diameters. Symbols are defined in the text.

			Angle to C axis (deg)						
Material	Diameter		0	15	30	45	60	75	90
		κ/T^3							
		(W cm^{-1} deg^{-4})	0.279	0.234	0.224	0.241	0.274	0.308	0.324
Cadmium	3 mm	Λ_{corr}/D	0.959	0.803	0.769	0.828	0.940	1.06	1.11
		A_κ	0.905	0.768	0.761	0.863	1.04	1.21	1.29
		κ/T^3							
		(W cm^{-1} deg^{-4})	8.98	8.82	8.77	9.24	7.96	7.05	6.81
Helium 4	1.773 mm	Λ_{corr}/D	1.06	1.04	1.03	1.09	0.939	0.831	0.803
		A_κ	1.22	1.20	1.18	1.22	1.01	0.864	0.821
		κ/T^3							
		(W cm^{-1} deg^{-4})	2.50	2.35	2.05	1.78	1.44	1.19	1.11
Thallium	3 mm	Λ_{corr}/D	1.57	1.47	1.28	1.11	0.902	0.744	0.692
		A_κ	2.14	1.98	1.63	1.31	0.959	0.728	0.655
		κ/T^3							
		(W cm^{-1} deg^{-4})	0.167	0.135	0.116	0.121	0.140	0.168	0.203
Zinc	3 mm	Λ_{corr}/D	1.09	0.880	0.753	0.785	0.913	1.10	1.32
		A_κ	1.01	0.824	0.719	0.795	1.01	1.30	1.60
		κ/T^3							
		(W cm^{-1} deg^{-4})	0.119	0.121	0.131	0.152	0.137	0.128	0.126
Zirconium	3 mm	Λ_{corr}/D	0.828	0.844	0.916	1.06	0.960	0.895	0.880
		A_κ	0.867	0.892	0.987	1.16	1.05	0.965	0.941

and the fast (normally L) mode, and thus can only occur in the slow (normally T_2) mode. For conditions in which the slow mode is quasilongitudinal and the fast mode is quasitransverse T_2, the slow longitudinal mode may have cuspidal edges. In this case the quasilongitudinal and the transverse T_1 mode, because of their lower velocity, will make the major contribution to the flow of heat. When cuspidal edges are present one should expect an enhanced phonon conductivity along those directions.

Listed in Table VI are the results of calculations to determine the phonon conductivity and the phonon-conduction-enhancement factor for five solids having strong focusing properties. Four of these solids have cuspidal edges, and one has two sets of cuspidal edges. The phonon conductivity of zirconium and helium 4, each having a cuspidal edge in the T_2 mode about θ_2, do indeed reach maximum in the vicinity of the cusp, the phonon-conduction-enhancement factors being 1.16 and 1.22, respectively. However, for helium 4, focusing of the T_1 mode about the C axis gives an enhancement factor as large as that near the cusp. In the case of cadmium and zinc, however, the phonon-conduction-enhancement factor along the C axis where high focusing is predicted is only 0.905 and 1.01, respectively, whereas along $C_\perp$ is 1.29 and 1.60, respectively. This is a direct result of the finite length-to-diameter ratio used in the calculations. For a sample length of only 10 rod diameters, phonons deviating as much as 6° from the sample rod axis can still travel nearly the entire length of the sample. But if the high-intensity portion of the phonon beam is confined to deviations of say 0.5° from the rod axis, the average phonon flux per unit area will be of the order of $(0.5)^2/(6)^2 \simeq 0.7\%$ of the average high-density portion of the beam. Under these conditions the average phonon flux per unit cross section could be comparable to that in an isotropic solid even though the high-intensity region be 150 times the isotropic intensity. Calculations for cadmium and zinc using longer samples yielded a sharp increase in the phonon-conduction-enhancement factor along the C axis. Except for the cusp in the T_2 mode for zinc about $C_\perp$, cadmium and zinc exhibit more modest focusing along $C_\perp$, but over a wide angle so that the total phonon flux along a rod axis parallel to $C_\perp$ actually exceeds the total flux along a rod axis parallel to the C axis. A more vivid example of modest wide-angle focusing is the case of thallium. The large phonon-enhancement factor along the C axis is due to focusing in the T_1 mode which is always cusp-free. In this case the phonon-enhancement factor along the C axis is more than three times the value along $C_\perp$.

The predictions of thermal conductivity for solid helium 4 appear in reasonable agreement with measurements of Hogan, Guyer, and Fairbank.[25] Careful comparison is difficult because the elastic constants vary significantly with molar volume and no measurements of the elastic constants have been reported for the molar volumes used in the thermal-conductivity experiments. Furthermore, the thermal-conductivity data do not follow a T^3 law above approximately 0.4 °K and few measurements were performed below this temperature. Finally, the thermal length of the crystals used in the experiments are not known. In view of these difficulties any reasonable agreement is encouraging.

Finally, note that focusing calculations already performed for crystals of lower symmetries indicate that phonon focusing is a general property of elastically anisotropic solids. Strong focusing is predicted to have a dramatic effect upon the phonon conductivity at very low temperatures. For dielectric solids this should be observable at temperatures which are a small fraction of the Debye temperature, but for superconductors this will not likely be observed until $T/T_c \ll 1$. These results, on completion, will be presented for publication at a later date.

ACKNOWLEDGMENTS

The author wishes to express his appreciation to the Worcester Area College Computation Center located on the campus of Worcester Polytechnic Institute for the use of its computing facilities. Appreciation is also extended to Professor Charles Elbaum for his critical reading of the manuscript.

[1]For a general review, see J. M. Ziman, *Electrons and Phonons* (Oxford U. P., London 1960); P. Carruthers, Rev. Mod. Phys. 33, 92 (1961); P. G. Klemens, in *Solid State Physics*, edited by F. Seitz and D. Turnbull (Academic, New York, 1958), Vol. 7, p. 1; Paper No. 66-9F5-TPROP-P5 (Westinghouse Research Laboratories Library, Pittsburgh, Pa. 1966) (unpublished).

[2]H. B. G. Casimir, Physica 5, 495 (1938).

[3]R. Berman, F. E. Simon, and J. M. Ziman, Proc. R. Soc. Lond. 220A, 171 (1953).

[4]R. Berman, E. L. Foster, and J. M. Ziman, Proc. R. Soc. Lond. 231A, 130 (1955).

[5]B. Taylor, H. J. Maris, and C. Elbaum, Phys. Rev. Lett. 23, 416 (1969).

[6]B. Taylor, H. J. Maris, and C. Elbaum, Phys. Rev. B 3, 1462 (1971).

[7]A. K. McCurdy, Ph.D. thesis (Brown University, 1971) (unpublished).

[8]H. J. Maris, J. Acoust. Soc. Am. 50, 812 (1971).

[9]A. K. McCurdy, H. J. Maris, and C. Elbaum, Phys. Rev. B 2, 4077 (1970).

[10]J. Bardeen, L. N. Copper, and J. R. Schrieffer, Phys. Rev. 106, 162 (1957); Phys. Rev. 108, 1175 (1957).

[11]A. C. Anderson, C. B. Satterthwaite, and S. C. Smith,

Phys. Rev. B 3, 3762 (1971).
[12]See, for example, L. D. Landau and E. M. Lifshitz, *Theory of Elasticity* (Addison-Wesley, Reading, Mass., 1959), p. 105.
[13]M. J. P. Musgrave, Proc. R. Soc. Lond. 226A, 356 (1954).
[14]F. I. Fedorov, *Theory of Elastic Waves in Crystals* (Plenum, New York, 1968), pp. 215–219.
[15]A mode will be considered quasitransverse if the angle between the polarization vector and the wave vector is greater than 45° but less than 135°.
[16]G. Arlt and H. Schweppe, Solid State Commun. 6, 783 (1968).
[17]Y. Ohmachi, N. Uchida, and N. Niizeki, J. Acoust. Soc. Am. 51, 164 (1972).
[18]Reference 14, p. 16.
[19]Reference 14, p. 124.
[20]This is true providing $C_{13}+C_{44}>0$. If $C_{13}+C_{44}<0$, there is an interchange of the two roots. There is no distinction between these two cases in the expressions for the phase velocity and the components of group velocity. Since it is physically more reasonable to assume $C_{13}+C_{44}>0$, this will be the only case considered in this paper.
[21]K. Brugger, J. Appl. Phys. 36, 759 (1965). Equation (17) agrees with Brugger.
[22]M. J. P. Musgrave, Proc. Cambridge Philos. Soc. 53, 897 (1957).
[23]See for example, N. B. Conkwright, *Introduction to the Theory of Equations*, (Ginn, New York, 1941), pp. 82, 78; J. V. Uspensky, *Theory of Equations* (McGraw-Hill, New York, 1948), p. 94.
[24]For cadmium the half-width of the cusp about the C axis is approximately 0.11° or $\theta_d/9$, so Eq. (56) does not give the correct amplification factor. In this case one must perform an exact integration over all wave vectors within the angle θ_{k2} about the C axis. The amplification factor becomes

$$A=\frac{1-\cos\theta_{k2}}{1-\cos\theta_d}\simeq\frac{2(1-\cos\theta_{k2})}{\theta_d^2}.$$

The angle θ_{k2} must be determined numerically. For cadmium and for an angle θ_d of 1°, the value of θ_{k2} is 8.743°.
[25]E. M. Hogan, R. A. Guyer, and H. A. Fairbank, Phys. Rev. 185, 356 (1969).
[26]J. DeKlerk, J. Phys. Chem. Solids 28, 1831 (1967).
[27]J. N. Fox, J. U. Trefny, J. Buchanan, L. Shen, and B. Bertman, Phys. Rev. Lett. 28, 16 (1972).